Calculation of stochastic premixed combustion in 1D porous burner with uncertainty in the convective heat transfer coefficient

J. L. Sereno, J. M. C.Pereira, J. C. F. Pereira *

Instituto Superior Tecnico,
Mech. Eng. Dept.,
Av. Rovisco Pais 1049 – 001 *Lisbon,*
Portugal

Abstract

Numerical calculations of one-dimensional premixed methane combustion in an inert porous burner subject to random variables are reported. The convective heat transfer coefficient was assumed to be a random variable and the stochastic process was represented using the polynomial chaos expansion. The combustion model consists of a global kinetic mechanism with transport equations for the fuel and oxidizer mass fractions with an Arrhenius source term. Two modelling assumptions are proposed for the stochastic transport equation with the Arrhenius source term. The used methodology allowed to quantify the uncertainty for the gas and solid temperatures due to a random heat transfer coefficient and to identify the locations where the uncertainty, characterized by the root mean square temperatures, presented higher values.

Key words: Porous Burner, Stochastic, Convective Heat Transfer Coefficient, Polynomial Chaos
PACS:

1 Introduction

Porous medium burners have received particular interest in the last decade due to some features such as high modulation range, high power intensity, low pollutants emissions and compact dimensions, see e.g. Trimis and Durst [2], Hsu and Matthews [1], Tien and Vafai [3] and Malico et al. [4]. The porous

* Corresponding Author: jcfpereira@ist.utl.pt

medium is, in most of the cases, made of ceramic foams and different materials have been used such as Al_2O_3 or SiC with porous dimensions ranging from 10 to 60 pores per inch (ppi). The porous materials have high porosities ($> 85\%$) and consequently low pressure losses are obtainned at high pore Reynolds numbers ($Re_d = \mathcal{O}[10^2]$), in the laminar regime.
Heat and mass transfer and combustion in porous media, at high pore Reynolds numbers in the laminar regime, embraces many modelling parameters with several uncertainty sources, see Kaviany [5] and Bejan and Nield [6]. The uncertainty inputs related with the porous structure, the geometry, the inlet and boundary conditions. In addition, there is the uncertainty of the modelling assumptions and in fluid and solid properties, conductivity, radiative properties, volumetric convective heat transfer coefficient, etc. To quantify how these uncertainties propagate it is necessary to know mean values, representing the most probable solution, and its error bar. This requires the introduction of new stochastic or random variables in the governing non-linear partial differential equations. The quantification of the uncertainty with standard Monte Carlo methods is prohibitive for most of the practical cases.
Traditionally the uncertainty in porous media was related with the porous geometry and with the solid void fraction. However, the ceramic foams have a quasi ordered structure with high porosity and consequently are far away from the geometrical uncertainty that characterises the stochastic porous media presented in complex geological environments and many statistical methods have been applied to Darcy flows, see e.g. Zhang [7] and Dodson and Thompson [8].
An important source of uncertainty in porous burners is the convective heat transfer coefficient because it appears in the source terms of the gas and solid energy equations and influences the equilibrium between the two phases. Due to the reactants preheating by the solid matrix it is possible to have superadiabatic temperatures in the porous burner. The thermal equilibrium between the solid and gas temperatures is dependent on the volumetric convective heat transfer coefficient that couples the energy equations for the gas and for the solid phases. The convective heat transfer coefficient has been experimentally and theoretically investigated by many authors and several proposed correlations are of type $Nu = cRe_d^m$ in which c and m are functions of d/l, being d the porous diameter and l the porous specimen thickness, and Prandtl number, see e.g. Fu et al. [9] and Howel et al. [10]. The proposed correlations should be valid within the measured range of parameters and their violation is responsible for a high uncertainty in porous burner models.
Recently, fluid and heat transfer stochastic problems have employed polynomial chaos expansions that are computationally faster alternatives to the prohibitive Monte Carlo method for multidimensional flow problems. Polynomial chaos is a member of the set of homogeneous chaos defined by Wiener [11]. The polynomial chaos expansions were introduced in the context of of partial differential equations by Ghanem and Spanos [12] and a set of papers were published concerning heat transfer conduction firstly by Ghanem [13] and later by Xiu and Karniadakis [14] among others. Uncertainty quantification due to

buoyancy effect has also been studied in Le Maitre et al. [15]. These studies provided important insight into the physics of the transport phenomenon and rich information was obtained about the thermal systems response to uncertainty. Reactive flows subjected to uncertainty inputs have been studied by Debuschere et al. [16] and Reagan et al. [17].
The objective of this work is to investigate the premixed combustion of CH_4 and air in an inert porous media subjected to a stochastic heat transfer coefficient. The approximation of the Arrhenius term in the scalar transport equations is discussed and a computational procedure is proposed to deal with stochastic transport equations with Arrhenius source terms. The proposed modelling assumptions are described and prior to the presentation of the main results, a validation of our numerical method is performed against reported stochastic solutions of heat transfer equations. This is followed by the presentation of the main results grouped in two subsections, corresponding the first to the heat source analogue and the second to the stochastic single step Arrhenius reaction modelling.

2 Numerical Method

In this section we present the governing equations and the polynomial chaos approach for the solution of systems of partial differential equations with random inputs. The porous burner model and the assumed properties for the fluid and solid matrix are also described.

2.1 Governing equations

The porous foam burner will be assumed to be one-dimensional and adiabatic. The one-step global reaction model for the combustion of a stoichiometric mixture of methane and dry air will be considered. The deterministic equations to model this problem are

Energy equation for the gas

$$\rho c_p \varepsilon A \frac{\partial T_f}{\partial t} + \rho u \varepsilon c_p A \frac{\partial T_f}{\partial x} = \frac{\partial}{\partial x}\left(k_f \varepsilon A \frac{\partial T_f}{\partial x}\right) + HA(T_s - T_f) + \Delta h_c \varepsilon A S_{fu} \tag{1}$$

Energy equation for the solid

$$\rho_s c_s (1-\varepsilon) A \frac{\partial T_s}{\partial t} = \frac{\partial}{\partial x}\left(k_s (1-\varepsilon) A \frac{\partial T_f}{\partial x}\right) + HA(T_f - T_s) \tag{2}$$

Transport equation for the fuel

$$\rho A \varepsilon \frac{\partial Y_{fu}}{\partial t} + \rho u \varepsilon A \frac{\partial Y_{fu}}{\partial x} = \frac{\partial}{\partial x}\left(\rho D_{AB} \varepsilon A \frac{\partial Y_{fu}}{\partial x}\right) - A\varepsilon S_{fu} \tag{3}$$

Transport equation for the oxidizer

$$\rho A \varepsilon \frac{\partial Y_{ox}}{\partial t} + \rho u \varepsilon A \frac{\partial Y_{ox}}{\partial x} = \frac{\partial}{\partial x}\left(\rho D_{AB} \varepsilon A \frac{\partial Y_{ox}}{\partial x}\right) - A\varepsilon S_{ox} S_{fu} \tag{4}$$

and the Ahrrenius term is given by

$$S_{fu} = A_r \rho^2 Y_{fu} Y_{ox} \exp\left(-\frac{E_a}{R_o T_f}\right) \tag{5}$$

where $A_r = 10^{10} m^3/kgs$ is the pre-exponential constant and $E_a = 1.4 \times 10^8 J/kmol$ is the activation energy for the methane. The heat source $\dot{Q}$ is either prescribed to simulate the heat release or assumed equal to $\dot{Q} = \Delta h_c \varepsilon A S_{fu}$ in case of premixed reaction flame. The inlet temperature boundary condition is of $300K$ for the solid and fluid phases. The burner consists of two porous media slices, the first is made of packed spheres with porosity $\varepsilon_1 = 0.26$ and the second is made of PSZ (partially stabilized ziconia) ceramic foam with a porosity $\varepsilon_2 = 0.87$. The length of the porous burner is $5cm$ being the first zone the pre-heating zone and the second zone is where the flame front is anchored. The flashback is avoided due to the low porosity of the upstream zone. The physical properties assumed are listed in table 1.

2.2 Polynomial chaos representation of stochastic processes

A random variable can be represented using the polynomial chaos (PC) expansion

$$X(\theta) = \sum_{i=0}^{\infty} a_n \Psi(\xi(\theta)) \tag{6}$$

Prop.	Media 1	Media 2	Dimensions
k_s	2	1	W/mK
ρ_s	3000	3000	kg/m^3
c_s	var.	var.	J/kgK
c_p	1000	1000	J/kgK
ε	$1-\pi/\sqrt{18}$	0.87	m^3/m^3
H	10^6	10^6	W/m^3K

Table 1
Porous burner properties.

where the functions $\Psi(\xi)$ for a complete orthogonal basis in the norm space defined by

$$\langle u, v\rangle = \int_S u(\xi)v(\xi)w(\xi)d\xi \tag{7}$$

where $w(\xi)$ denotes the weighting function. The Wiener-Askey family of orthogonal polynomials is defined by weight functions that are similar to probability density functions, see Karniadakis [18] for details. A general differential equation with stochastic inputs can be represented by

$$F(x, t, \theta, u) = f(x, t, \theta) \tag{8}$$

The equation above must be projected into the space spanned by the polynomial basis defined earlier in order to absorb the random variables and to minimize the representation error. Only the P+1 terms of the series in equation 6 will be retained. This procedure leads to

$$\left\langle F\Big(x, t, \xi, \sum_{i=0}^{P} u_i\Psi_i\Big), \Psi_k \right\rangle = \left\langle f(x, t, \xi), \Psi_k \right\rangle \tag{9}$$

The dimension of this system of equations depends on the dimension of the random vector n and on the number of approximation modes P

$$(P+1) = \frac{(n+p)!}{n!p!} \tag{10}$$

This means that instead of solving one differential equation with random inputs one has to solve a system of coupled deterministic equations. It is important to note that we first restrict the solution space to contain separable functions, relieving afterwards by considering an expansion with sufficient number

of stochastic modes. Applying this procedure to the standard transport equation we obtain

$$\frac{\partial \phi_k}{\partial t} + \frac{1}{\|\Psi_k\|^2} \sum_{i=0}^{P} \sum_{j=0}^{P} e_{ijk} U_i \frac{\partial \phi_j}{\partial x} = \frac{1}{\|\Psi_k\|^2} \sum_{i=0}^{P} \sum_{j=0}^{P} e_{ijk} \frac{\partial}{\partial x} \left(\Gamma_i \frac{\partial \phi_j}{\partial x} \right) + S_k(x,t) \tag{11}$$

where the term $S_k(x,t)$ is the projected source term given by the following equation

$$S_k(x,t) = \frac{1}{\|\Psi_k\|^2} \int_{\Omega} S(\phi(\xi)) \Psi_k(\xi) w(\xi) d\xi \tag{12}$$

The gas energy equation terms are approximated, term by term, by:

$$\rho c_p \varepsilon(\omega) A \frac{\partial T_f(\omega)}{\partial t} \equiv c_p A \sum_{i=0}^{P} \sum_{j=0}^{P} \sum_{m=0}^{P} e_{ijmk} \rho_i \varepsilon_j \frac{\partial T_{f(m)}}{\partial t} \tag{13}$$

$$\dot{m} c_p \frac{\partial T_f(\omega)}{\partial x} \equiv \dot{m} c_p \frac{\partial T_{f(k)}}{\partial x} \|\phi_k\|^2 \tag{14}$$

$$\frac{\partial}{\partial x} \left(k_f \varepsilon(\omega) A \frac{\partial T_f(\omega)}{\partial x} \right) \equiv \sum_{i=0}^{P} \sum_{j=0}^{P} e_{ijk} \frac{\partial}{\partial x} \left(k_f \varepsilon_i A \frac{\partial T_{f(j)}}{\partial x} \right) \tag{15}$$

$$H(\omega) A (T_s(\omega) - T_f(\omega)) \equiv A \sum_{i=0}^{P} \sum_{j=0}^{P} e_{ijk} H_i T_{s(j)} - A \sum_{i=0}^{P} \sum_{j=0}^{P} e_{ijk} H_i T_{f(j)} \tag{16}$$

The terms of the solid phase energy equation appear as

$$\rho_s c_s (1 - \varepsilon(\omega)) A \frac{\partial T_s(\omega)}{\partial t} \equiv \rho_s c_s A \frac{\partial T_{s(k)}}{\partial t} \|\phi_k\|^2 - \rho_s c_s A \sum_{i=0}^{P} \sum_{j=0}^{P} e_{ijk} \varepsilon_i \frac{\partial T_{s(j)}}{\partial t} \tag{17}$$

$$\frac{\partial}{\partial x} \left(k_s (1 - \varepsilon(\omega)) A \frac{\partial T_s(\omega)}{\partial x} \right) \equiv \frac{\partial}{\partial x} \left(k_s A \frac{\partial T_{s(k)}}{\partial x} \right) \|\phi_k\|^2 - \sum_{i=0}^{P} \sum_{j=0}^{P} e_{ijk} \frac{\partial}{\partial x} \left(\varepsilon_i A \frac{\partial T_{s(j)}}{\partial x} \right) \tag{18}$$

$$H(\omega)A(T_f(\omega) - T_s(\omega)) \equiv A\sum_{i=0}^{P}\sum_{j=0}^{P} e_{ijk}H_i T_{f(j)} - A\sum_{i=0}^{P}\sum_{j=0}^{P} e_{ijk}H_i T_{s(j)} \quad (19)$$

The scalar transport equation, for example, for the fuel mass fraction appears as

$$\rho A\varepsilon(\omega)\frac{\partial Y_{fu}(\omega)}{\partial t} \equiv A\sum_{i=0}^{P}\sum_{j=0}^{P}\sum_{m=0}^{P} e_{ijmk}\rho_i\varepsilon_j\frac{\partial Y_{fu(m)}}{\partial t} \quad (20)$$

$$\rho u\varepsilon(\omega)A\frac{\partial Y_{fu}(\omega)}{\partial x} \equiv \dot{m}\frac{\partial Y_{fu(k)}}{\partial x}\|\phi\|^2 \quad (21)$$

$$\frac{\partial}{\partial x}\left(\rho D_{AB}\varepsilon(\omega)A\frac{\partial Y_{fu}(\omega)}{\partial x}\right) \equiv A\sum_{i=0}^{P}\sum_{j=0}^{P}\sum_{m=0}^{P} e_{ijmk}\frac{\partial}{\partial x}\left(\rho_i D_{AB}\varepsilon_j A\frac{\partial Y_{fu(m)}}{\partial x}\right) \quad (22)$$

The Arrhenius source becomes

$$S_{fu(k)} = \frac{1}{\|\phi_k\|^2}\int_{\Omega} S_{fu}(\rho(\xi), Y_{fu}(\xi), Y_{ox}(\xi), T_f(\xi))\phi_k(\xi)w(\xi)d\xi \quad (23)$$

and will be modeled by two different assumptions. In the first, which is referred to as an approximate Arrhenius representation (S_{fu} approximation), it was assumed that this term only varies with the first mode of the temperature, which means that it only varies with the mean solution. The second approximation, which we denominate complete Ahrrenius representation (S_{fu} complete) consists of using Least-Squares approximation of $S_{fu}(\xi)$ using the orthogonal polynomials as the basis of functions and obtaining the coefficients directly. A collocation method was used as in Balakrishnan [21] where higher order mode zeros were used to minimize the error.
The computational grid has a constant grid spacing at the flame front and expands geometrically to the boundaries. This assures that the flame will not stabilise due to numerical disspation. The density is calculated using the perfect gas law and the invertion of the temperature in the equation requires the solution of a linear system of equations to obtain the stochastic modes (see Debsscherre et al. [19]):

$$\rho T_f = const. \quad (24)$$

$$\sum_{i=0}^{P}\sum_{j=0}^{P} e_{ijk}\rho_i T_{f(j)} = const.\delta(k)\|\phi_k\|^2 \quad (25)$$

The strongly coupled system of equations was discretized by an implicit scheme together with central finite differences approximation for the spatial derivatives. The solution error is due to the space and time numerical discretization

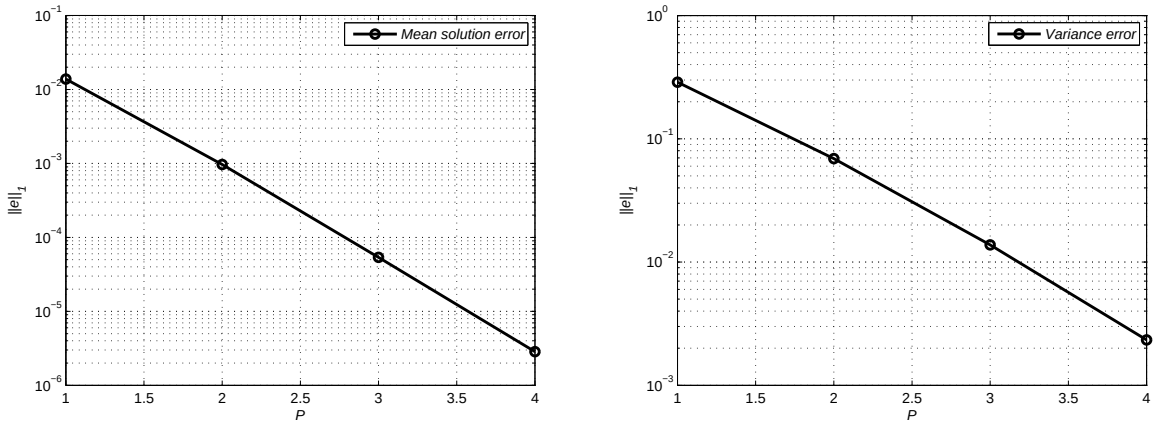

Figure 1. Solution error for the mean (Left) and the variance (Right)

and the approximation error of the random process. Before the presentation of the solutions for the porous burner combustion under random inputs, some remarks considering the accuracy of the numerical model can be made recurring to a much simpler model equation:

$$\frac{dy(t)}{dt} = ky(t) \tag{26}$$

with the initial condition $y(0) = 1$ and k is considered a Gaussian random variable with zero mean and a unit variance. This equation was investigated by Karniadakis et al. [18] with a similar numerical model. The projection of this equation leads to the following system of equations for the several modes

$$\frac{dy_k(t)}{dt} = \frac{1}{\|\Psi_k\|^2} \sum_{i=0}^{P} \sum_{j=0}^{P} e_{ijk} k_i y_j(t) \tag{27}$$

where e_{ijk} is given by

$$e_{ijk} = \int_{\Omega} \Psi_i \Psi_j \Psi_k w(\xi) d\xi \tag{28}$$

The system of equations was solved by a 2^{nd} order Runge-Kutta method as in Karniadakis et al. [18]. Figure 1 shows that the error in the mean and in the variance decreases almost one order of magnitude per additional stochastic mode denoting a very fast convergence. Figure 2 shows the error obtained from the calculated theoretical variance and the numerical variance error obtained with the numerical method and several meshes. A saturation effect occurs when the numerical discretization error is of the same order of magnitude of the stochastic mode approximation error.

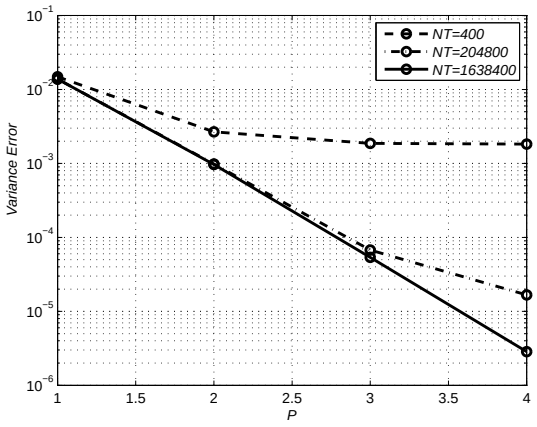

Figure 2. Predicted and obtained variance error $||e||_1$.

The one-dimensional heat conduction model subjected to a random diffusivity α is also a test case of interest for the present study. The previously applied procedure yields the system of $(P+1)$ one-dimensional heat equations for the different modes

$$\frac{\partial T_k}{\partial t} = \frac{1}{\|\Psi_k\|^2} \sum_{i=0}^{P} \sum_{j=0}^{P} e_{ijk} \alpha_i \frac{\partial}{\partial x} \left(\frac{\partial T_j}{\partial x} \right) \tag{29}$$

The diffusivity was considered to be a Gaussian random variable with $\alpha \sim N(1/2, \sqrt{11}/2)$. The initial conditions are given by:

$$T_k(t=0,x) = \begin{cases} A \sin\left(\frac{\pi x}{L}\right) & k = 0 \\ 0 & k \neq 0 \end{cases} \tag{30}$$

where A is the initial amplitude and was set to be equal to one. The exact solution for this problem is

$$T(t,x) = A \frac{(-1)^k (\alpha_1 t)^k}{k!} \left(\frac{\pi}{L}\right) e^{\pi^2 t \frac{(\alpha_1^2 \pi^2 t - 2\alpha_0 L^2)}{2L^2}} \sin\left(\frac{\pi x}{L}\right) \tag{31}$$

Since the diffusivity was modeled by a Gaussian random variable, meaning that $P[X < 0] \neq 0$, this solution is unbounded and consequentely without physical nature.

The system of equations 29 were solved considering several modes recurring to a 2^{nd} order spacial discretization scheme and a first order implicit method. The numerical error is presented in figure 3 for the mean solution and its variance. The results show that for a fixed numerical resolution, the approximation error may become independent of the number of stochastic modes (see figure 3). This does not mean that a converged solution was not obtained, it only means

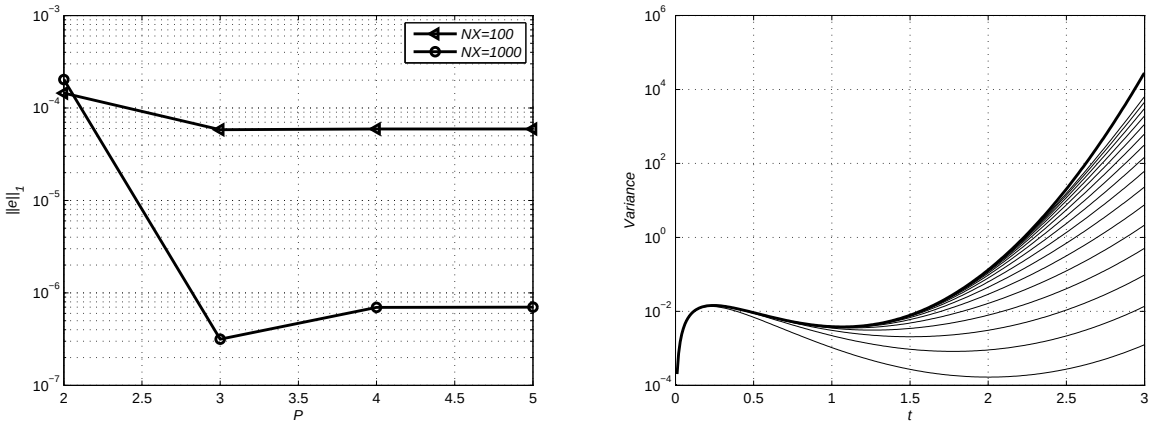

Figure 3. Convergence of the mean solution for the one-dimensional transient diffusion test case (Left) and predicted successive approximations for the solution variance (Right).

that a better numerical resolution is needed for a more accurate solution to be obtained.

3 Results

The system of gas and solid energy equations and species concentration equations were solved by a central differences for the diffusion terms and upwind differences for the convective terms together with the implicit Euler scheme. A mesh comprising $NX = 659$ grid points was used with a uniform region located at the flame front. The convective heat transfer coefficient was considered to be a random variable. Heat release was modeled either by a prescribed heat source or a one-step reaction model of the premixed combustion. The power of the porous burner was $7.5kW$ for a stoichiometric premixed reaction of methane and air. The random heat transfer coefficient was characterised assuming a Gaussian random variable with a variability coefficient (rms to mean value ratio) of 20% and a mean value of $10^6 \quad W/m^3K$.

3.1 Heat source analog

A heat source was prescribed in the gas energy equation with a source distribution given in figure 4. The predicted mean temperature profiles are represented in figure 5. The maximum heat release is obviously at the precribed position $x = 3cm$, at the interface of the two porous mediums. The upstream fluid is pre-heated because of the conduction heat transfer (and radiation in real cases) due to the solid matrix. The uncertainty, quantified by the tempera-

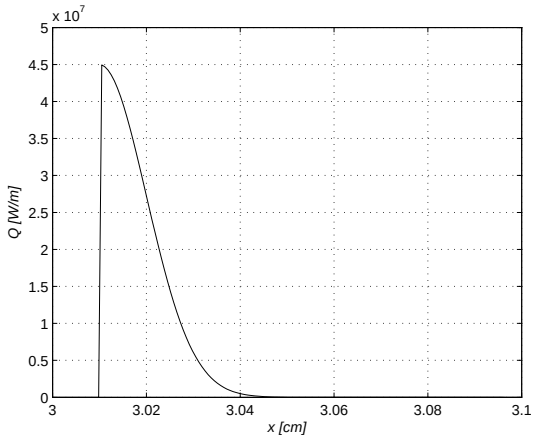

Figure 4. Prescribed heat source profile.

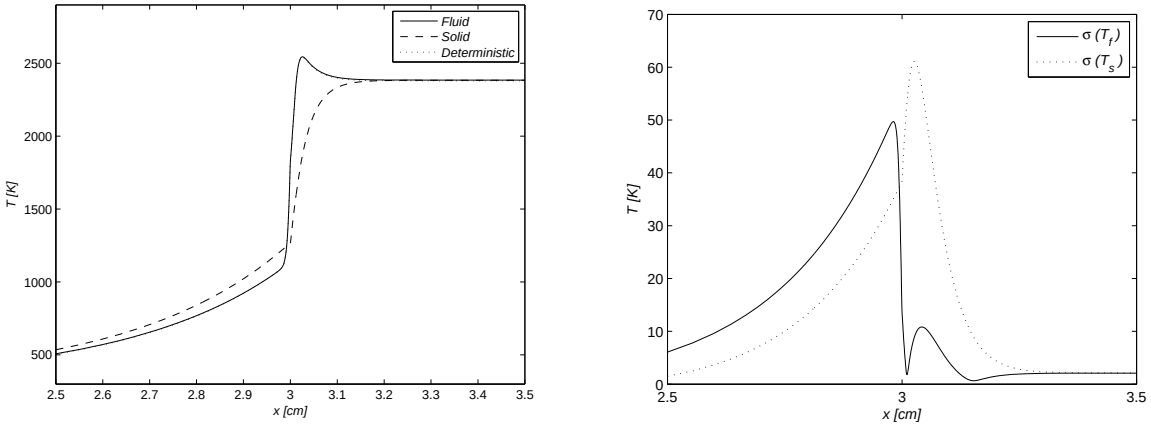

Figure 5. Mean temperatures (Left) and standard deviations (Right) for the prescribed heat source test case.

ture standard deviation, increases gradually in the preheating zone achieving a maximum of $50K$, falling abruptly at the interface of the two porous media. This is caused by different porosities and conduction coefficients. After the interface zone the uncertainty increases slightly because there is still heat transfer between the solid and the gas. Has soon as the solid and gas are in equilibrium the uncertainty in the temperature becomes very low and constant. The maximum of the standard deviation for the gas and for the solid temperatures are not coincident due to thermal inertia. Figure 7 shows the calculated mean density and the standard deviation. The successive approximations of the density standard deviation show virtual identical results, validating the selected methodology based on equation 25 and indicating that four modes were enough for a good respresentation of the stochastic space.
Another test case was performed considering that both the porosity ε and the convective heat transfer coefficient were independent Gaussian random variables with 5% and 20% variability coefficients, respectively. The same

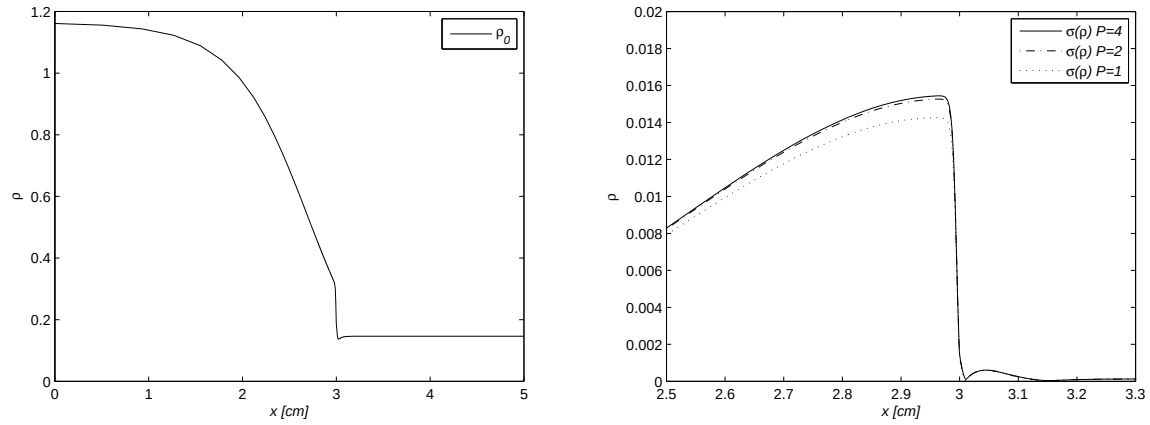

Figure 6. Mean density (Left) and standard deviation (Right) for the prescribed heat source test case $[kg/m^3]$.

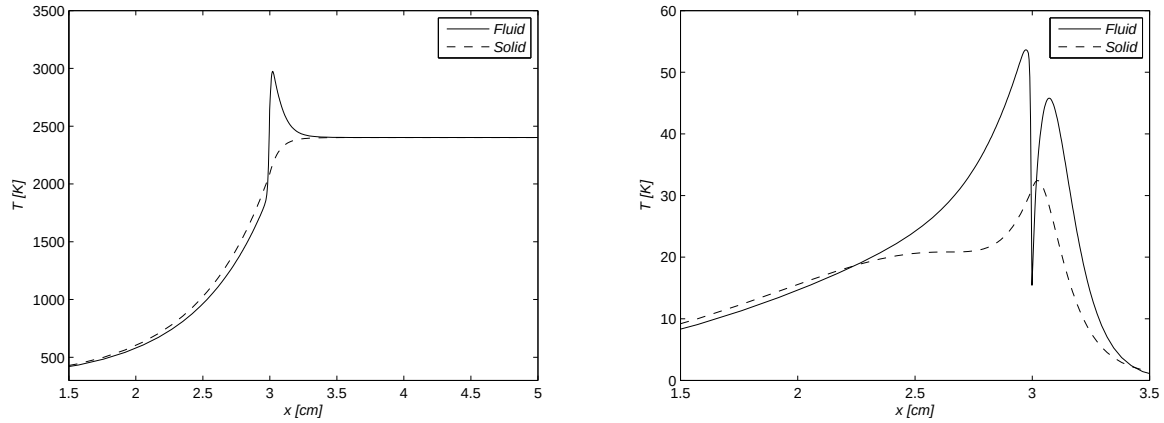

Figure 7. Mean temperatures (Left) and standard deviation (Right) for the two-dimensional random input case.

heat source was prescribed for comparison purposes. The predicted mean and standard deviations obtained are represented in figure 7. The predicted mean temperatures are too high because of the prescribed heat source analog of the premixed flame heat release and due to neglecting radiation. Nevertheless it is possible to investigate the qualitative influence of the two simultaneous stochastic variables on the temperature field. The effect of adding the porosity as a stochastic variable is to increase the preheating zone temperature and to reduce the solid temperature uncertainty and to increase the uncertainty of the gas temperature. This is specially notorious downstream of the porous interface.

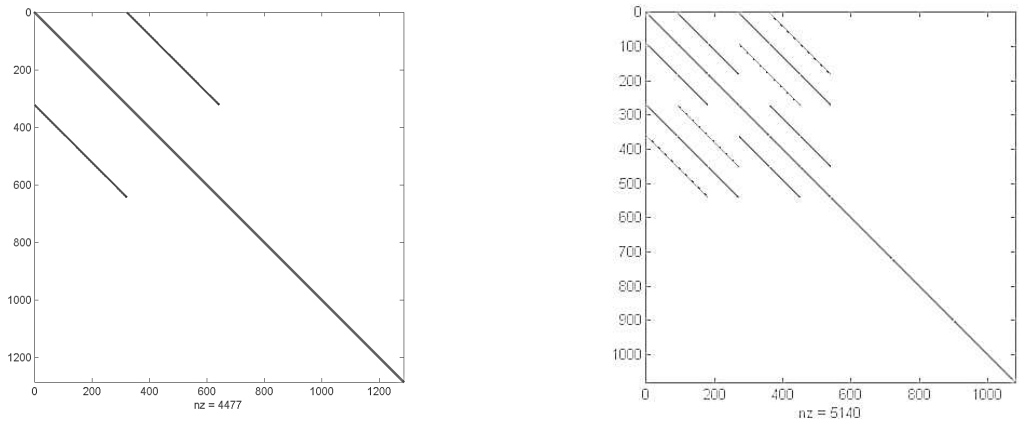

Figure 8. Sparsity patterns for the deterministic (Left) and the stochastic (Right) problems.

3.2 Stochastic one-step combustion model

The deterministic system of four coupled partial differential equations originate, after the projection procedure, a system of $4(P+1)$ coupled PDE's. A first order implicit temporal discretization was used together with first order upwind differences for the convective terms and second order central differences for diffusion terms. The numerical stabilisation of this scheme was obtained with a pseudo-transient technique (only steady state solutions are sought).
A relative error of 0.1% was found between the temperature obtainned with two non uniform grid comprising $NX = 659$ and $NX = 1414$ points together with an approximation of $P = 2$. Usually a 200 grid point approximation is enough to obtain a good representation of the deterministic case but for the stochastic case the higher order stochastic modes also need to have a better resolution. The numerical difficulties arising from this system of equations comes from its stiffness and from the type of approximation used for the Arrhenius term. All the terms were treated as implicit, except for the Arrhenius term because of its effect on the matrix condition number and spectrum. The global matrix is represented for the deterministic and stochastic case with an approximation of $P = 3$ in figure 8. The matrix corresponding to the stochastic problem comprises diagonal (convection) and tridiagonal blocks (diffusion terms) corresponding to the coupling between the solid and gas temperatures for each modes. The strong coupling of the system of equations, for each mode, prevents a segregate solution to be efficient. The Jacobi pre-conditioning accelerated the iterative process and the resulting system of equations was solved using the *GMRES* solver based on Krylov subspace approximations, see e.g. Marques and Pereira [20] for details. Figure 9 shows an example of the matrix spectrum with and without pre-conditioning for $P = 2$ and a coarse mesh. As expected the eigenvalues for the preconditioned matrix form a group around

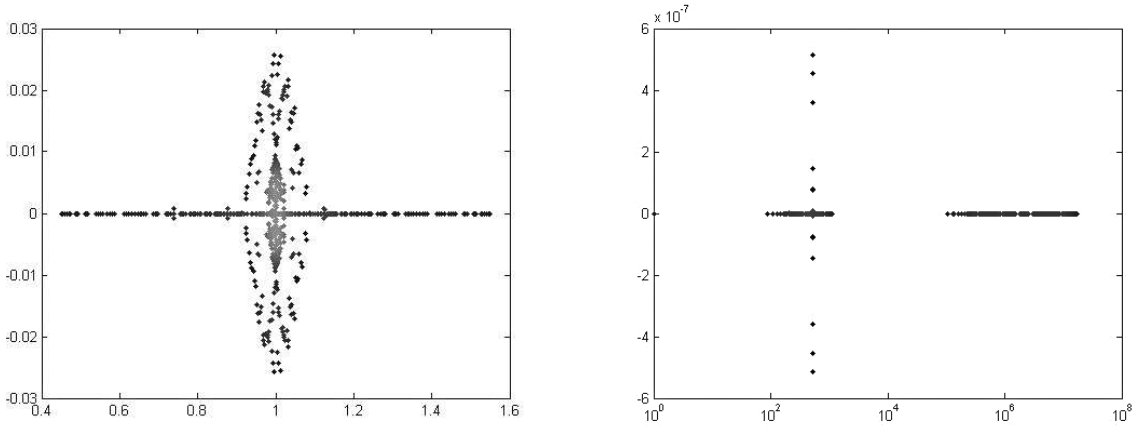

Figure 9. Matrix spectrums for the deterministic (Left) and the stochastic (Right) problems.

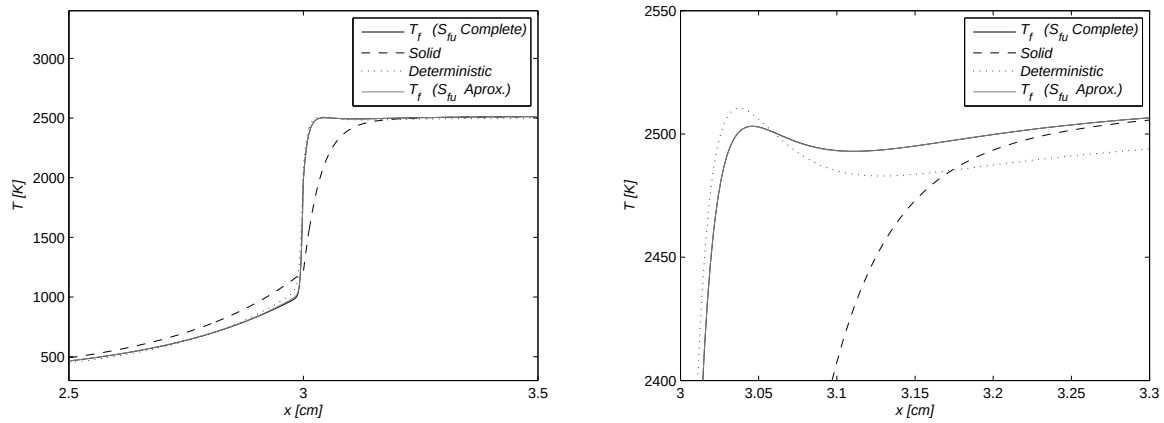

Figure 10. Mean and deterministic temperature profiles for the solid and fluid.

unity and the condition number is reduced from 10^7 to 10^0.

The Ahrrenius term for the stochastic modes was approximated with two different strategies.

For the present calculations a random heat transfer coefficient was assumed with a Gaussian 20% variability, as before. Figure 10 shows the mean solid temperature and the mean fluid temperature obtained with the S_{fu} complete model and with the S_{fu} approximation model. Both approaches yield the same mean temperature. This shows that the mean solution is not greatly affected by the source terms higher order modes.

The mean temperature is slightly different from the deterministic temperature and there is more pre-heating in the deterministic solution than in the stochastic solution and consequently the flame deterministic temperature has a higher peak than the stochastic case. However the mean stochastic solution corresponds to the statistical average of many realizations and consequently there is no physical phenomena associated with the ensemble mean. The only physical meaning is that the most probable temperature distribution is shown

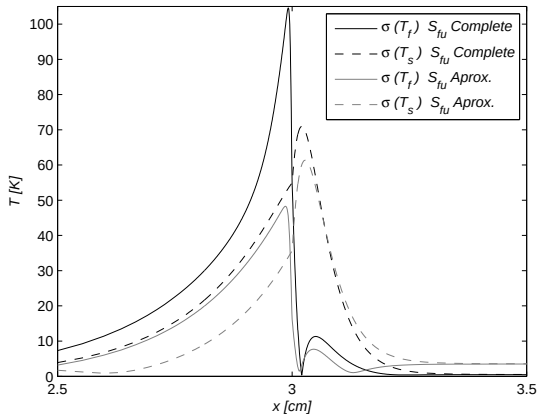

Figure 11. Solid and fluid temperature standard deviation.

in figure 10.

Figure 11 shows the root mean square of the temperature that quantifies the uncertainty of the gas and solid temperatures for the S_{fu} complete and aproximate models. The approximate Arhenius model (S_{fu} approximate) predicts that the maximum standard deviation occurs in the solid temperature reaching a peak of $60K$. It can be seen that the pre-heating zone plays an important role on the initial increase of the uncertainty. Downstream the interface the uncertainty in the fluid temperature decreases sharply due to the change in the characteristic porous size. The standard deviation of the fluid and solid temperature becomes approximately equal after the flame front because the magnitude of the term $H(T_f - T_s)$ decreases. This term acts as the uncertainty source for this system. It is interesting to note that the approximate Ahrrenius model (S_{fu} approximation) gives predictions of the temperature standard deviation in close agreement with the heat source analog case, see figure 5 because of the uncoupling of the source term with the different modes.

In the complete Ahrrenius approximation (S_{fu} complete), the complete polynomial chaos expansion is calculated. The results for the mean temperature are represented also in figure 10. One important remark is that the approximation considered earlier gives an excellent estimate for the mean solution,being the two lines virtually coincident. On the other hand it can be seen in figure 11 that this does not happen with the standard deviations. The uncertainty is underestimated by the approximate representation model (S_{fu} approximation) that predicts that the maximum standard deviation for the temperatures occurs in the solid phase,what is, in fact, wrong. The maximum standard deviation obtainned with S_{fu} complete is of $100K$ which almost doubles the prediction of the approximate model. The pre-heating region and flame front region are very important for the growth of the uncertainty. Comparing these results with the previous approximation, where there was no coupling of the Ahrrenius term with the higher order modes, one concludes that this term amplifies the uncertainty through its non-linear behaviour. The fact that the approximate model is able to represent accurately the mean solution makes possible to calculate

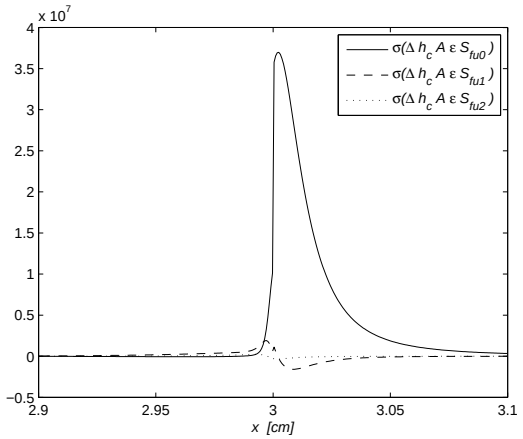

Figure 12. Source term stochastic modes.

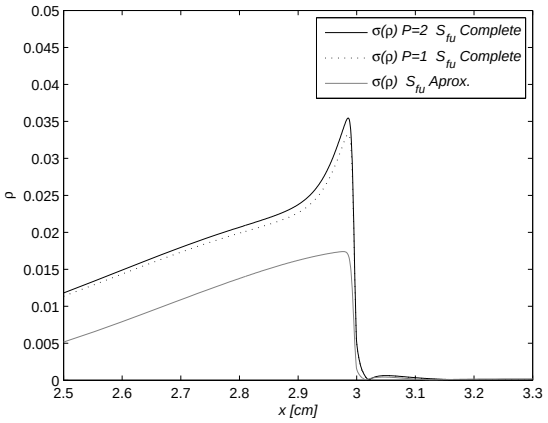

Figure 13. Fluid density stochastic modes $[kg/m^3]$.

first the steady state approximate solution (with lower computational effort) and then apply the complete model to capture the higher order modes which are related to higher order statistics (variance, skewness, kurtosis, ...).
Figure 12 shows that the stochastic modes of the source term and higher order terms are quite different from the first (mean) mode. The inability of the approximate model (S_{fu} approximation) to capture the higher order behaviour of this physical system is also present in the standard deviation of the density of the fluid (see figure 13). The uncertainty related to this quantity is also underestimated by the (S_{fu} approximation). This error may be related to the fact that we introduce an unbalance in the system when we use different approximation levels for the Arrhenius term and the global system.
The approximate Ahrrenius term predicts that the uncertainty in the mass fractions are only important in the region of the flame front (figure 14). The standard deviations of the mass fractions are also underestimated by the approximate model. Furthermore the complete model (S_{fu} complete) predicts a less localized phenomena with relatively large uncertainty upstream and

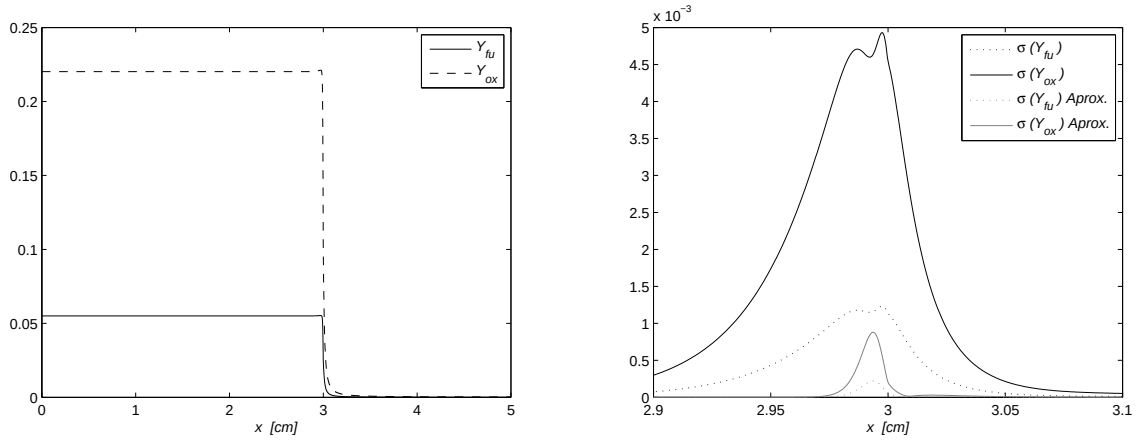

Figure 14. Fuel and oxidizer mass fractions (Left) and standard deviations (Right).

downstream to the flame front.

4 Conclusions

The stochastic 1D energy equation for the gas and solid phases and scalar species transport equations were solved considering the polynomial chaos expansion to represent the stochastic processes. The flame heat release was modeled by 1D premixed reactive flow in inert porous media with the inclusion of the one-step global Ahrrenius source term and the mass fraction scalar transport equations. A very simple source analogue model requiring only the energy equations with a prescribed source was also considered to describe the heat transfer process.

Calculations of previously reported simple stochastic differential equations show the mutual influence of the numerical error inherent to the spacial and temporal discretizations and the number of polynomial chaos expansion modes. The calculations provide excellent agreament with the benchmark test cases.

A porous burner was calculated assuming two degrees of approximation of the Ahrrenius term. In the first, we assumed that this term depended only in the mean variables. This approximation lead only to a good representation of the mean solution and underestimated the uncertainty expressed by the standard deviation of the temperature field. The second model corresponds to a complete model which is based in a Least-Squares/Colocation method. The complete Ahrrenius representation with three stochastic modes allowed a good accuracy of the stochastic solution and showed that for a random heat transfer coefficient the uncertainty is created in the pre-heating zone and in the flame region, being also convected downstream.

References

[1] Hsu, P.F. and Matthews, R.D., 1993, The necessity of using detailed chemical kinetics in model for premixed combustion in porous media, Combustion and Flame, 93, 457-466. 5

[2] Trimis, D. and Durst, F., 1996, Combustion in porous medium advances and applications, Combustion Science and Techknowlogy, 121, 153-168.

[3] Tien, C.L., and Vafai, K., 1989, Convective and radiative heat transfer in porous media, Advances in Applied Mechanics, 27, 607-632.

[4] Malico, Isabel, Zhou, X.Y., Pereira, J.C.F., 2000, Two-dimensionoal numerical study of combustion and pollutants formation in porous burners, Combustion Science and Techknowlogy, 152, 57-79.

[5] Kaviany, M., Princeiples of Heat Transfer in Porous Media, 2nd Edition, Springer Verlag, 1995.

[6] Bejan, A., Nield, B.A., Convection in Porous Media, 2nd Edition, Springer Verlag, New York, 1999.

[7] Zhang, D., Stochastic Methods for Flow in Porous Media, Academic Press, 2001.

[8] Dodson, C.T.J., and Sampson, W.W., Flow simulation in stochastic porous media, Simulation, 74:6, 351-358, 2000.

[9] Fu, X., Viskanta, R., Gore, J.P., 1998, Measurement of volumetric heat transfer coefficient of cellular ceramics, Exp. Ther. Fluid Sci., 17, 285-293.

[10] Howell, J.R., Hall, M.J., Ellzey, J.L., 1996, Combustion of hydrocarbon fuels within porous inert media, Progress in Energy and Combustion Science, 22(2):121-145.

[11] Wiener, N., 1938, The Homogeneous Chaos, Amer. Jour. Math., 60, 897-936.

[12] Ghanem, R., Spanos, P., Stochastic Finite Elements: A Spectral Approach, Springer-Verlag, 1991.

[13] Ghanem, R., 1999, Higher order sensitivity of heat conduction to random data using the spectral stochastic finite element method, Journal of Heat Transfer Transactions of ASME, 121(2): 290-299.

[14] Xiu, D., Karniadakis,G., 2003, A new stochastic approach to transient heat conduction modeling with uncertainty, Int. Jour. Heat and Mass Transfer, 46, 4681-4693.

[15] Le Maitre, O.P., Knio, O.M., Debusschere, B.J., Najm, H.N. and Ghanem, R.G., 2001, A stochastic projection method for fluid flow, Journal of Computational Physics, 173, 481-511.

[16] Debusschere, B.J., Najm, A.N., Matta, A., Knio, O.M., Ghanem, R.G., Le Maitre, O.P., 2003, Protein labelling reactions in electrochemical microchanel flow: Numerical simulation and uncertainty propagation, Physics of Fluids, 8, 2238-2250.

[17] Reagan, M.t., Najm, A.N., Debusschere, B.J., Le Maitre, O.P., Bert, J., Knio, O.M., Ghanem, R.G., 2004, Spectral stochastic uncertainty quantification in chemical systems, SIAM, Jour. Sci. Comput., 8, 607-632.

[18] Xiu, D., Karniadakis, G., 2002, The Wiener-Askey polynomial chaos for stochastic differential equations, SIAM, 24(2):612-644.

[19] Debusscherre, B.J., Najm, A.N., Pebay, P.P., Knio, O.M., Ghanem, R.G., Le Maitre, O.P., 2004, Numerical Challenges in the use of polynomial chaos representations of stochastic processes, SIAM, Jour. Sci. Comp., 26, 689-719.

[20] Marques, N., Pereira, J.C.F., 2004, Comparison of matrix-free acceleration techniques in compressible Navier-Stokes equations calculations, Int. Jour. of Num. Meth. Eng., 61(3):455-476.

[21] Balakrishnan, S., Georopoulos, P., Benerjee, I., Ierapetritou, M., 2002,Uncertainty considerations for describing complex reaction systems, AIChE, 48(12):2875-2889.